

FILLING THE REGION BETWEEN VERTICAL COAXIAL CYLINDERS
OF AN ANOMALOUSLY VISCOUS FLUID UNDER NONISOTHERMAL CONDITIONS

V. K. Bulgakov, A. M. Lipanov, and K. A. Chekonin

UDC 532.522:518.12

We offer a calculation algorithm for the flow of an anomalous viscous fluid with a free surface in the region between vertical coaxial cylinders. The influence of nonisothermal conditions of filling this region is demonstrated with respect to the nature of the hydrodynamic process.

Among the numerous types of non-Newtonian fluid flows exhibiting practical application for analysis of the technological processes involved in the treatment of polymer materials, of particular importance are those flows with a free surface. Despite the urgency of the problem of numerically modeling the complex flows of full nonlinear viscoplastic media, the initial efforts along these lines appeared only very recently [1, 2]. This is explained by the difficulty of solving the problem because of the nonlinear properties of the fluids, the complexity of achieving specific boundary conditions at the free surface, as well as because of the nonisothermicity of the process and the existence of anomalies near the solid surfaces (the Π -effect).

I. Let us examine the nonisothermal flow of a non-Newtonian incompressible fluid with a free surface between vertical coaxial tubes. We will take the equations from the mechanics of continuous media with the rheological Shul'man model [3] as the basis of our mathematical description of the process. We take into consideration four basic factors which enable us to obtain correct results: the nonlinear relationship between the stress tensor and the strain rates, the relationship between the rheological constants and temperature, the dissipation of the energy of motion, and the slippage that occurs at the solid boundaries.

Thus the problem of the flow of an anomalous viscous fluid with a free surface, filling a given region Ω , reduces to the determination of the region Ω_t over time, as well as of the velocity vector \mathbf{V} and of the pressure vector p , as well as of the non-Newtonian viscosity μ , satisfying the following in this region:

the continuity equation

$$\frac{\partial v_3}{\partial x_3} + \frac{1}{x_1} \frac{\partial (x_1 v_1)}{\partial x_1} = 0, \quad (1)$$

the equations of motion

$$\begin{aligned} \rho \left(\frac{\partial v_1}{\partial t} + v_1 \frac{\partial v_1}{\partial x_1} + v_3 \frac{\partial v_1}{\partial x_3} \right) &= - \frac{\partial p}{\partial x_1} + \mu \left(\Delta v_1 - \frac{v_1}{x_1^2} \right) + \\ &+ 2 \frac{\partial \mu}{\partial x_1} \frac{\partial v_1}{\partial x_1} + \frac{\partial \mu}{\partial x_3} \left(\frac{\partial v_1}{\partial x_3} + \frac{\partial v_3}{\partial x_1} \right), \quad (2) \\ \rho \left(\frac{\partial v_3}{\partial t} + v_1 \frac{\partial v_3}{\partial x_1} + v_3 \frac{\partial v_3}{\partial x_3} \right) &= - \frac{\partial p}{\partial x_3} + \frac{\partial \mu}{\partial x_1} \left(\frac{\partial v_1}{\partial x_3} + \frac{\partial v_3}{\partial x_1} \right) + \\ &+ \mu \Delta v_3 + 2 \frac{\partial \mu}{\partial x_3} \frac{\partial v_3}{\partial x_3} - \rho g, \end{aligned}$$

the equation of energy

All-Union Pumping Machinery Technological Scientific Research Institute, Kazan'. Translated from *Inzhenerno-Fizicheskii Zhurnal*, Vol. 57, No. 4, pp. 577-583, October, 1989. Original article submitted April 13, 1988.

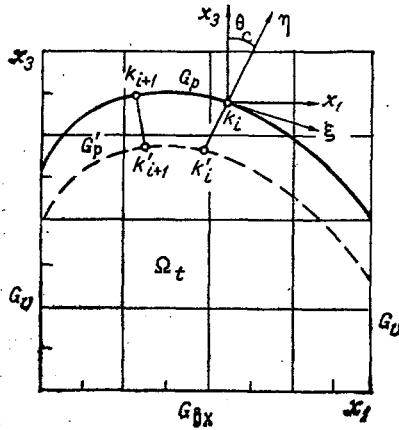


Fig. 1. The shape and boundaries of the occupied region.

$$\rho c_p \left(\frac{\partial T}{\partial t} + v_1 \frac{\partial T}{\partial x_1} + v_3 \frac{\partial T}{\partial x_3} \right) = \left[\frac{\partial}{\partial x_1} \left(\lambda x_1 \frac{\partial T}{\partial x_1} \right) + \frac{\partial}{\partial x_3} \left(\lambda x_1 \frac{\partial T}{\partial x_3} \right) \right] x_1^{-1} + \mu A^2, \quad (3)$$

where $\mu = [\tau_0^{1/n} + (\mu_p A)^{1/m}] n A^{-1}$ is the non-Newtonian viscosity [3].

The equations are written in a cylindrical coordinate system ($x_1 = r$, $x_3 = z$) for the axisymmetric case.

The temperature relationship of the rheological parameters is assumed to be of the following form [3-5]:

$$\mu_p = \mu_p(T_0) \exp P n_1, \quad \tau_0 = \tau_0(T_0) \exp P n_2. \quad (4)$$

On solution of the basic equations (1)-(3), for the boundary conditions we will use:

1. At the solid boundaries G_v (Fig. 1):

$$v_1 = 0, \quad v_3 = v_{s1}, \quad T_w = \text{const}. \quad (5)$$

2. At the inlet G_{in} specifies the velocity profile for the steady-state flow of a Newtonian fluid in the region between coaxial cylinders [4]:

$$v_3 = \frac{2Q}{\pi R_2^2} \left[1 - \left(\frac{x_1}{R_2} \right)^2 + \frac{\beta^2 - 1}{\beta^2 \ln \beta} \ln \frac{x_1}{R_2} \right] \left(\frac{\beta^4 - 1}{\beta^4} - \left(\frac{\beta^2 - 1}{\beta^2} \right)^2 / \ln \beta \right)^{-1}, \quad v_1 = 0, \quad (6)$$

for the temperature

$$T|_{G_{in}} = T_0. \quad (7)$$

Boundary condition (6) does not correspond to the distribution of the velocity in the steady-state flow of the medium with Shul'man rheology; however, because of the smallness of the initial hydrodynamic segment the boundary condition (6) exerts no significant influence on the hydrodynamic process.

3. At the free surface G_p (Fig. 1), moving in agreement with the kinematic condition:

$$\left. \frac{dx_1}{dt} \right|_{G_p} = v_1, \quad \left. \frac{dx_3}{dt} \right|_{G_p} = v_3, \quad (8)$$

the dynamic boundary condition reflects the equality of normal stress arising within the medium to the given external pressure above the free surface (p_n) and to the absence of tangential stress. In our case this condition can be represented in the form

$$\mathfrak{s}^3 R \cdot \mathfrak{s}^3 = -p_n, \quad \mathfrak{s}^1 \cdot R \cdot \mathfrak{s}^3 = 0. \quad (9)$$

Here R is the stress tensor, $\mathfrak{s}^1, \mathfrak{s}^3$ are the unit vectors of the local coordinate system (ξ, η), connected to the free boundary. With solution of Eq. (3) we impose on G_p the adiabatic condition

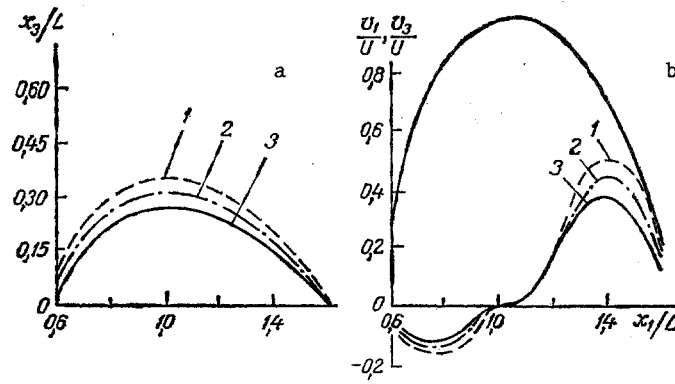


Fig. 2. The influence exerted by the temperature gradient in the region of solid boundaries: a) on the location of the free surface; b) on the velocity profile of the free boundary; 1) $\Delta T = 60^\circ\text{C}$; 2) 30; 3) 0.

$$\left. \frac{\partial T}{\partial \eta} \right|_{\sigma_p} = 0. \quad (10)$$

To determine the pressure we use the Poisson equation which is derived from the equation of motion (2), with consideration given to the continuity equation (1), and it has the form

$$\Delta p = 2 \left(\frac{\partial \mu}{\partial x_1} \Delta v_1 + \frac{\partial \mu}{\partial x_3} \Delta v_3 + \frac{\partial^2 \mu}{\partial x_1^2} \frac{\partial v_1}{\partial x_1} + \frac{\partial^2 \mu}{\partial x_1 \partial x_3} \left(\frac{\partial v_1}{\partial x_3} + \frac{\partial v_3}{\partial x_1} \right) + \frac{\partial^2 \mu}{\partial x_3^2} \frac{\partial v_3}{\partial x_3} \right) - \rho \left(\frac{2}{x_1} \frac{\partial^2 (x_1 v_1 v_3)}{\partial x_3^2} + x^{-2} \frac{\partial^2 (x_1 v_1)}{\partial x_1^2} \right). \quad (11)$$

The boundary conditions for the pressure at the inlet and at the solid walls are determined also from the equation of motion (2), in conjunction with the continuity equation (1).

II. All of the differential equations and boundary conditions are written in finite-difference form on a rectangular grid of fixed nodes (20×60), covering the entire flow region. This is a first-order approximation. In the vicinity of the free surface the basic finite-difference equations are solved on an irregular grid. Here, as was demonstrated in [6], instead of the boundary-value problem (1)-(10), we can solve the boundary-value problem (2)-(11), but in this case we require satisfaction of the continuity equation at the boundaries G_{in} , G_v , G_p (Fig. 1), which guarantees conservation of the velocity field within the region. As the initial conditions of the problem we specify the fields of velocity, pressure, temperature, and effective viscosity, obtained through numerical integration of Eqs. (2)-(11) for the case of a plane free surface. For the solution of the difference analogs of Eqs. (2), (3), and (11) we use the adaptive procedure of the SOR method [7]. To reduce the errors in determining the position of the free boundary at the surface, we introduce particle markers. Their position in the subsequent time interval is determined from the kinematic condition (8). The shape of the free surface is approximated by means of cubic splines from the found coordinate of the particle markers.

A fundamental difficulty in solving the problem is the numerical realization of the boundary conditions at the free surface. For the solution we will use the method proposed in [6, 8], where in order to satisfy conditions (1) and (9) on the free surface they are combined for the local coordinate system (ξ, η) into the following invariant form of the equations:

$$\begin{aligned} \frac{\partial N}{\partial \eta} + \frac{\partial N}{\partial \xi} + \frac{S}{R_s} + \frac{v_1}{x_1} &= 0, \\ \frac{\partial S}{\partial \eta} - \frac{\partial S}{\partial \xi} + \frac{N}{R_s} + \frac{v_1}{x_1} &= 0. \end{aligned} \quad (12)$$

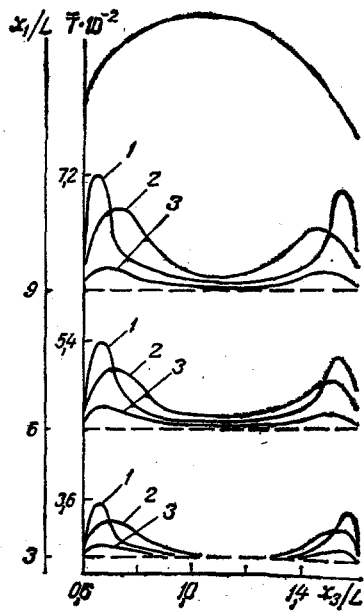


Fig. 3. Evolution of the temperature profile in the region of the flow for the case in which $T_0 = T_w$: 1) $Se = 5 \cdot 10^{-3}$; $Re = 2.6 \cdot 10^{-6}$; $Pr = 2.5 \cdot 10^7$; $n/m = 1.88$; 2) $7.6 \cdot 10^{-2}$; $8.6 \cdot 10^{-5}$; $4.2 \cdot 10^5$ and 1.38 ; 3) 0.43 ; $9.4 \cdot 10^{-4}$; $3.3 \cdot 10^5$ and 1.1 .

Here $N = v_\eta + v_\xi$, $S = v_\eta - v_\xi$, v_η and v_ξ are the components of the velocity vector in the local coordinate system; R_s is the curvature radius of the free boundary. To determine the implicit functions S and N we construct an additional iteration process whose unique features are to be found in [1, 9]. When the region Ω is filled with a non-Newtonian fluid with $\tau_0 > 10$ Pa and large mean-mass flow rates $Q/S_0 > 1.3 \cdot 10^{-3}$ m/sec the free surface exhibits a clearly defined convexity ($H/L > 0.5$). The numerical calculations showed that the best results under these filling conditions are obtained if the approximation of Eqs. (9) and (12) is accomplished with an equidistant G_p curve (to the surface), passing through the regular nodes of the Euler grid (Fig. 1). The normals to G_p are drawn from the points k_i' , situated on G_p' , with an approximately equal interval $h < \Delta x_1$. The value of the velocity components at the points k_i' are calculated by interpolation between the values of the local fluid velocity in the nodes of the adjacent cells, and these are found in advance by a numerical method. Having determined the values of N_k and S_k , we find the components of the velocity vector at the points k_i of the free surface

$$(v_\xi)_k = (N_k - S_k)/2, (v_\eta)_k = (N_k + S_k)/2. \quad (13)$$

The components $(v_1)_k$ and $(v_3)_k$ are determined on the basis of the formulas for the transition from the local coordinate system (ξ, η) to a global coordinate system (x_1, x_3) :

$$\begin{bmatrix} v_1 \\ v_3 \end{bmatrix}_k = \begin{bmatrix} \cos \theta_k & -\sin \theta_k \\ \sin \theta_k & \cos \theta_k \end{bmatrix} \begin{bmatrix} v_\xi \\ v_\eta \end{bmatrix}_k. \quad (14)$$

The pressure values at the point k are determined from the difference analog of the first equation in system (9). To find the values of u , v , and p in the regular nodes of the grid, we require appropriate interpolation.

The algorithm for the solution of the problem thus involves the following:

on the basis of the difference analogs of Eqs. (2)-(11) we determine the pressure and the velocity components within the region in the $(n + 1)$ -th iteration, and the value of the non-Newtonian viscosity in this case is taken from the n -th iteration;

from the different analogs of Eqs. (8) and (9) we determine the velocity vector and the pressure at the free surface in the $(n + 1)$ -th iteration;

substituting these values of the components of the velocity vector into the finite-difference energy equation (3), we determine the temperature field within the flow region;

from the found temperature field and from relationships (4) we determine the value of the limit fluidity and plastic viscosity;

after convergence of the iteration process, on the basis of the difference analogs of the kinematic condition (7) we find the new position of the free surface;

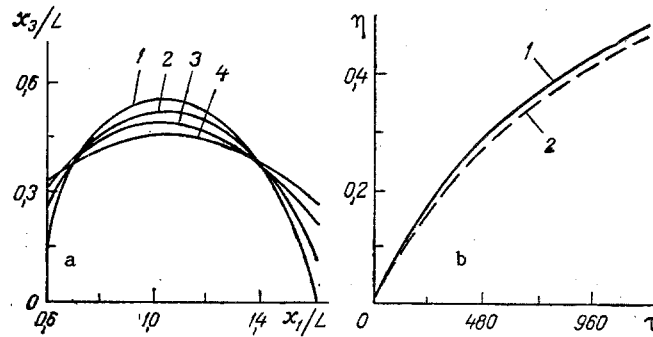


Fig. 4. Evolution of the shape of the free surface under the action of the force of gravity; 1) $\tau = 0$; 2) 714; 3) 3000; 4) 5430; a) change in the discharge parameter of the cylindrical column of a viscoplastic fluid ($h_0/r_0 = 1.7$) during the time ($\mu_p = 407 \text{ Pa}\cdot\text{sec}$; $\tau_0 = 1.5 \text{ Pa}$; $n = 1$; $m = 1.8$; $\rho = 1500 \text{ kg/m}^3$; 1) experiment; 2) theory) (b).

in the derived region Ω_t we again find the solution of Eqs. (2), (3), and (11).

Equations (2)-(11) were solved in dimensionless form. For our dimensions we have taken the distance between the external and internal cylinders $L = R_2 - R_1$, the mean discharge velocity U , the effective viscosity $\mu_{\text{eff}} = [\tau_0^{1/n} + (\mu_p A_m)^{1/m}]^n A_m^{-1}$ and the initial temperature T_0 of the medium. The criterial relationships that are formed in this case are of the form: $Re = \rho UL / \mu_{\text{eff}}$, which is the effective Reynolds number; $Pr = \mu_{\text{eff}} / (\rho a)$, which is the effective Prandtl criterion; and $Fr = U^2 (gL)^{-1}$, which is the Froude number.

To determine the rate of wall slippage at the solid boundaries G_V we employed the empirical relationships given in [9-12]:

$$\begin{aligned} (v_{s\dot{\theta}})_{R_1} &= \left[\frac{1}{2R_1} \left(\frac{\partial p}{\partial x_3} \right)_{R_1} (R_1^2 - R_{\text{cor}}^2) k_{\text{co}}^{-1} \exp Pn_s \right]^{1/s} U^{-1}, \\ (v_{s\dot{\theta}})_{R_2} &= \left[\frac{1}{2R_2} \left(\frac{\partial p}{\partial x_3} \right)_{R_2} (R_{\text{cor}}^2 - R_2^2) k_{\text{co}}^{-1} \exp Pn_s \right]^{1/s} U^{-1}. \end{aligned} \quad (15)$$

Here R_{cor} , $\partial p / \partial x_3$ is the radius of the flow core and the pressure gradient at the solid boundaries, determined through numerical solution of the stated problem; k_{co} , s are the empirical constants of the medium.

III. As an example of calculating the axisymmetric flow of an anomalous viscous fluid, let us examine the process of filling the region between vertical coaxial cylinders of dimensions $R_1 = 0.0084 \text{ m}$, $R_2 = 0.022 \text{ m}$. The rate of flow for the non-Newtonian medium with rheological parameters $\mu_p(T_0) = 50\text{-}5000 \text{ Pa}\cdot\text{sec}$; $n = 0.85\text{-}1.0$; $m = 0.53\text{-}1.6$ and $\tau_0(T_0) = 0\text{-}15 \text{ Pa}$ amounted to $Q = 1.14 \cdot (10^{-10}\text{-}10^{-5}) \text{ m}^3/\text{sec}$. The empirical constants of relationships (4) and (15), as well as the thermophysical characteristics of the medium were taken to be equal to $b_1 = 0.021 \text{ deg}^{-1}$, $b_2 = 0.0189 \text{ deg}^{-1}$, $b_3 = 0.038 \text{ deg}^{-1}$, $k_{\text{co}} = 2.25 \cdot (10^{10}\text{-}10^{16}) \text{ N}\cdot\text{sec}/\text{m}^{s+2}$, $s = 0.536$, $c_p = 1253 \text{ J}/(\text{kg}\cdot\text{deg})$, $\lambda = 0.09\text{-}0.46 \text{ J}/(\text{m}\cdot\text{sec}\cdot\text{deg})$. For a more complete description of the results from the numerical studies we will make use of the dimensionless complex $W = Re/Pr$ and the viscoplasticity parameter $Se = \tau_0 (\mu_{\text{eff}} A_m)^{-1}$.

Figure 2a shows the influence exerted by the temperature gradient in the region of the solid boundaries on the shape of the free surface in the case of $Re = 1.19 \cdot 10^{-8}$, $Pr = 3.5 \cdot 10^7$, $Se = 0.7$, $W = 18$. The coordinate origin for x_3 is found at the point of contact between the free surface and the wall of the outside cylinder. It follows from an analysis of the calculations that the increase in the temperature gradient in the region of solid boundaries $G_V(T_0 > T_w)$ leads to an increase in the tangential stresses and, as a consequence, to a more convex form of the free surface. In this case, the profiles of the axial and radial components of the velocity vector on the free surface have a form such as that shown in Fig. 2b.

To evaluate the influence of nonisothermicity in the hydrodynamic process due to the dissipative heating of the medium in the presence of various rheological parameters, Fig. 3 shows the development of the temperature profile over the length of the flow region ($T_w = T_0$). From the results of the numerical calculations it follows that for the above-specified

flow regime the dissipative heating is significant only for expanding media: $n/m > 1.2$, $\mu_p > 3000 \text{ Pa}\cdot\text{sec}$, and $\tau_0 > 13 \text{ Pa}$. It should also be noted that failure to take into consideration conditions (15) leads to a loss of medium mass up to 15% at $x_3 = 3L$.

When the region Ω is only partially filled by media exhibiting a fluidity limit, of importance is the determination of the shape of the free surface at the instant at which the influx of the following portion begins. Figure 4a shows the process of establishing the shape of the free surface under the action of its own weight, after cessation of the inflow of the medium with rheological parameters $\mu_p = 3200 \text{ Pa}\cdot\text{sec}$, $n = 1.0$, $m = 1.69$, $\tau_0 = 10 \text{ Pa}$, and a temperature gradient $T_0 - T_w = 20^\circ\text{C}$ at the walls. It follows from an analysis of the numerical studies that within the interval of time under consideration here the shape of the free surface undergoes considerable changes. In this case, a medium which exhibits a limit of fluidity, retains its convex shape. However, the influence of the temperature gradient on the solid boundaries (within limits of 10°C) exerts no significant influence on the hydrodynamic process under consideration.

Thus the nonisothermal conditions of filling a region with an anomalous viscous fluid, said region located between vertical coaxial cylinders, and the presence of the Π -effect at the walls may significantly affect the nature of the hydrodynamic process. Thus, the increase in the flow rate (Q) of the medium or of its rheological parameters τ_0 , μ_p , n/m leads to a more intensive dissipative heating of the medium and to a rise in the pressure drop across the wall region, and consequently it also leads to an increase in the slippage rate (v_{s1}). We should take note of their significant influence as early as the initial temperature gradient $T_0 - T_w = 20^\circ\text{C}$ at the walls and for filling regimes with $Re > 1 \cdot 10^{-6}$ when $Se > 5 \cdot 10^{-3}$.

To monitor the accuracy of the calculations, we undertook a test calculation of the nonisothermal discharge of a cylindrical column of non-Newtonian fluid when $T_0 = 40^\circ\text{C}$, $T_a = 20^\circ\text{C}$ (Fig. 4b) as well as calculations at the subsequent grids, and in addition we found the value of the difference analog for the divergence of the velocity vector in the cells of the grid. These calculations demonstrated the fact that the difference analog of the divergence was negligibly small in comparison with the average rate of fluid flow through the elementary cell [13-16].

NOTATION

v_1, v_3 , radial and axial components of the velocity vector; τ_0 , fluidity limit; ρ , density; n, m , constants of the rheological Shul'man model; g , acceleration of the force of gravity; R_1, R_2 , radii of the internal and external cylinders; e_{ij} , strain rate tensor; $A = \sqrt{2e_{ij}e_{ij}}$, intensity of strain rate; $A_m = U/L$, mean shear velocity; T , temperature; c_p , specific heat capacity; λ , coefficient of thermal conductivity; $a = \lambda(\rho c_p)^{-1}$, coefficient of thermal diffusivity; T_w , cylinder wall temperature; T_a , temperature of the ambient medium; $Pn_1 = b_1(T_0 - T)$, $Pn_2 = b_2(T_0 - T)$, $Pn_3 = b_3(T_w - T)$, dimensionless complexes taking into consideration the relationship between the rheological properties of the fluid and the non-isothermicity of the hydrodynamic process; b_1, b_2, b_3 , constants of the medium; $\eta = (r_t - r_0)/r_0$, discharge parameter; τ , time referred to $(\mu_p/(\rho g r_0))^{n/m}$; r_0 , initial radius of the cylindrical fluid specimen; r_t , maximum radius of the specimen at the given instant of time; H , maximum convexity of the free surface; Δx_1 , interval of the finite-difference grid in the radial direction; $\bar{T} = (T - T_0)/T_0$.

LITERATURE CITED

1. V. P. Ishchenko and A. N. Kozlobrodov, *Izv. SO Akad. Nauk SSSR, Ser. Tekh.*, Issue 2, No. 10, 34-42 (1985).
2. I. K. Berezin, *Investigating the Flow and Phase Conversion in Polymers Systems* [in Russian], Sverdlovsk (1985), pp. 10-15.
3. Z. P. Shul'man, *Convective Heat and Mass Transfer of Non-Newtonian Fluids* [in Russian], Moscow (1975).
4. D. M. MacKelvy, *Processing of Polymers* [Russian translation], Moscow (1965).
5. Z. P. Shul'man, Ya. N. Kovalev, and É. A. Zal'tsgendler, *The Rheophysics of Conglomerated Materials* [in Russian], Minsk (1978).
6. I. M. Vasenin, A. P. Nefedov, and G. R. Shrager, *Chisl. Met. Mekh. Splosh. Sred.*, 16, No. 6, 28-43 (1985).
7. L. Heigeman and D. Young, *Applied Iteration Methods* [Russian translation], Moscow (1986).

8. I. M. Vasenin, O. B. Sidonskii, and G. R. Shrager, Dokl. Akad. Nauk SSSR, 217, No. 2, 295-298 (1974).
9. V. K. Bulgakov and K. A. Chekhonin, The Youth of Udmurtiya - Accelerating the Scientific Engineering Process [in Russian], Izhevsk (1987), pp. 130-132.
10. N. I. Basov and V. Broi (eds.), Techniques in the Processing of Plastics [in Russian], Moscow (1985).
11. K. K. Trilinskii, Heat and Mas Transfer [in Russian], Vol. 2, Minsk (1972), pp. 363-367.
12. V. M. Gorislavets, A. A. Dunets, and G. N. Klyumel', Heat and Mass Transfer, Vol. 3 [in Russian], Minsk (1972), pp. 115-123.
13. V. P. Pervadchuk, V. A. Zelenkin, and V. A. Kaufman, Strength and Hydraulic Characteristics of Machines and Structures [in Russian], Perm' (1974), pp. 33-37.
14. N. E. Kochin, I. A. Kibel', and N. V. Roze, Theoretical Hydromechanics [in Russian], Vol. 2, Moscow (1963).
15. V. Vazov and G. Forsythe, Difference Methods for the Solution of Partial Differential Equations [Russian translation], Moscow (1963).
16. W. L. Wilkinson, Non-Newtonian Fluids [Russian translation], Moscow (1964).

AN ENERGY-BASED JUSTIFICATION FOR AND A COMPARISON OF THE METHODS
OF TECHNICAL-ECONOMIC AND ENERGY OPTIMIZATION OF CONVECTIVE
HEAT-EXCHANGE SURFACES

N. M. Stoyanov

UC 536.24:66.045.1

Calculation relationships are offered and a comparison is carried out of the energy and technical-economic optimization of these methods, and the limitations imposed on the latter are also established.

We currently have on hand a tremendous volume of theoretical and experimental material dealing with studies into the convective exchange of heat in the forced motion of coolants through channels exhibiting a variety of surface shapes. Among the most urgent problems are those connected with selection of the most effective heat-exchange surfaces, as well as the determination of their optimum operating conditions in the nominal regime.

The most objective comparison of convective heat-exchange surfaces and their optimization, in our opinion, is offered by the energy method which essentially involves determining the relationship between the intensity of the convective heat exchange and the specific expenditures of power on the propulsion of the coolant through the channels of the heat-exchange surface, and namely:

$$\alpha = f\left(\frac{N}{F}\right). \quad (1)$$

These specific expenditures can be determined from the relationship

$$\frac{N}{F} = \xi \frac{Re^{2.5} \nu \rho}{8d_{eq}^3}. \quad (2)$$

If for purposes of calculating the coefficient ξ we use the theoretical or empirical relationships of the form

$$\xi = \frac{A}{Re^m}, \quad (3)$$